

Kinetic stabilization of Fe film on GaAs(100): An *in situ* x-ray reflectivity Study

T. C. Kim, Y. Kim, and D. Y. Noh

Department of Materials Science and Engineering,

Gwangju Institute of Science and Technology, Gwangju 500-712, Korea

J.-M. Lee and S.-J. Oh

School of Physics & Center for Strongly Correlated Materials Research,

Seoul National University, Seoul 151-742, Korea

J.-S. Kim

Department of Physics, Sook-Myung Women's University, Seoul 140-742, Korea

(Dated: February 6, 2008)

Abstract

We study the growth of the Fe films on GaAs(100) at a low temperature, 140 K, by *in-situ* UHV x-ray reflectivity using synchrotron radiation. We find rough surface with the growth exponent, $\beta_S = 0.51 \pm 0.04$. This indicates that the growth of the Fe film proceeds via the restrictive relaxation due to insufficient thermal diffusion of the adatoms. The XRR curves are nicely fit by a model with a uniform Fe film, implying that the surface segregation and interface alloying of both Ga and As are negligible. When the Fe film is annealed to 300 K, however, the corresponding XRR can be fit only after including an additional layer of 9 Å thickness between the Fe film and the substrate, indicating the formation of ultrathin alloy near the interface. The confinement of the alloy near the interface derives from the fact that the diffusion of Ga and As from the substrate should proceed via the inefficient bulk diffusion, and hence the overlying Fe film is kinetically stabilized.

PACS numbers: 68. 55. -a, 68. 35. Fx, 68. 35. Ct

Recently, the ferromagnetic metal-semiconductor heterostructures has drawn intense attention for their application to the spintronic devices such as spin-polarized field effect transistors and spin-polarized light emitting diodes.¹ Such spintronic devices require highly polarized spin source and efficient spin injection through the interface of the heterostructures. The Fe/GaAs system has been studied as a prototype of the heterostructures, because high quality, epitaxial bcc Fe films can be grown on GaAs surfaces due to their small lattice mismatch only by $\sim 1.3\%$ ^{2,3}. Moreover, the spin injection from the Fe film into GaAs(100) has been realized even at room temperature⁴. However, the system still has enjoyed limited success, because the magnetic polarization of the Fe film and in turn spin injection efficiency has suffered from serious degradation due to the formation of nonmagnetic or antiferromagnetic Fe alloys with Ga and especially As outdiffused from the bulk^{5,6,7}.

There have been several attempts to suppress the alloy formation: sulfuric passivation of GaAs surface⁸, insertion of thin interlayer such as Er layer between Fe film and GaAs⁹. Those methods have reduced the outdiffusion and alloy formation of Ga and As, but the segregated As atoms have been still observed at the surface⁹. Y. Chye *et al*¹⁰ grow the Fe film on GaAs(100) at a low temperature (~ 120 K) and find improved magnetic properties of the Fe film such as the improved squareness. The alloy formation seems suppressed. However, structural and chemical analysis to confirm the assumed growth behavior of Fe/GaAs(100) at the low temperature has not been investigated. Only recently, photoelectron spectroscopy has been performed for the Fe film grown on GaAs(100) at 130 K and suggested that the alloy formation and outdiffusion of both Ga and As should be effectively suppressed.¹⁴

In the present work, we study the growth and thermal stability of the Fe films grown on GaAs(100) at 140 K by *in situ* x-ray reflectivity (XRR) study. The film has revealed the surface width developing with the growth exponent $\beta \approx 0.50$, reflecting the restricted relaxation processes at low temperature¹¹. Most of all, we find the formation of virtually pristine Fe film on GaAs(100) at 140 K. Further, the Fe film shows thermal stability against annealing up to 300 K, except the interface region of 9 Å thickness where the alloy forms. The confinement of the interface alloy is ascribed to the inefficiency of bulk diffusion process by which Ga and As diffuse into the Fe film.

All the experiments are performed in an ultrahigh vacuum (UHV) x-ray scattering chamber at 5C2 beam line of Pohang light source (PLS). The base pressure of the chamber is below 8×10^{-10} Torr. The GaAs(100) sample is of square shape with its lateral size 10

mm and thickness 0.6 mm. Clean GaAs(100) is obtained by several cycles of 0.5 keV Ar⁺ ion sputtering with the incident angle of 45° from the surface normal around 300 K and annealing up to 850 K. The sample temperature is monitored by both an optical pyrometer and a K-type thermocouple attached near the sample.

In order to observe the evolution of the surface morphology upon Fe deposition, specular XRR is measured. For the experiment, UHV chamber mounted on four-circle diffraction goniometer (2+2 mode) is employed. The incident x-ray is vertically focused by a mirror and monochromatized to a wavelength $\lambda = 1.239\text{\AA}$ by a double bounce Si(111) monochromator.

A commercial electron beam evaporator (EFM3, Omicron) is used to evaporate Fe (purity of 99.99%) at the rate of 0.026 Å/sec. During the deposition, the chamber pressure is maintained below 1×10^{-9} Torr and the substrate is held at 140 K. The deposition of Fe and the XRR measurement is alternated, and the referred thickness t of the Fe film is the accumulated amount of the deposited Fe. Since the Fe film does not follow layer-by-layer growth mode at 140 K, t is a nominal value.

Fig. 1 shows the specular XRR curves as a function of the out-of-plane momentum transfer, q_z . In each curve, the contribution from diffuse scattering was measured and subtracted. For the clean GaAs(100), reflected intensity is observed for very large q_z , which indicates small surface width, W_S . After curve fitting according to Parratt's formula,¹² W_S is found to be 2.01 ± 0.40 Å.

As the Fe film becomes thick, however, the slope of the specular XRR curve becomes steep, implying that the surface becomes rough. Thus, the XRR curves show very weak modulation because the constructive interference of the x-rays reflected from the rough surface (Vacuum/Fe) and those reflected from the rough interface (Fe/GaAs) hardly occurs. To assess the roughness of the film quantitatively, we again applied the Parratt's formula to fit the observed XRR curves. The fitting parameters include the effective electron density in the film, ρ , the thickness of the film, t , the width of the surface, W_S , and that of the interface, W_I . W_S (W_I) is defined as the root mean square of the height fluctuations at the surface (interface)¹³.

Each solid line in Fig. 1 represents the best fit of the experimental specular XRR curve obtained for the Fe film grown on GaAs(100) at 140 K. The model is composed of the homogeneous single Fe film on GaAs(100) and well reproduces the experimental XRR curves. (Fig. 1) The interface alloy and the segregated As-derived layer need not to be invoked

for the fit, suggesting that no significant chemical reactions of the Fe with the Ga and As occurs. The best-fit model is also consistent with the observation of the recent photoelectron spectroscopy that finds effective suppression of the outdiffusion of both Ga and As, and negligible interface alloying for the Fe film grown on GaAs(100) at 130 K¹⁴.

In Fig. 2, summarized are the W_S and W_I as a function of t . The linear dependence of the W_S and W_I on t in a double logarithmic scale implies a power law behavior, $W_{S,I} \sim t_{S,I}^\beta$, where β_S and β_I are 0.51 ± 0.04 and 0.37 ± 0.03 , respectively. Different β for each interface indicates that the surface roughness does not result from the propagation of the interface roughness or there is working different growth mechanism for the roughening process on each interface.

A simple model, random deposition without lateral relaxation¹⁵ gives rise to the $\beta \approx 0.50$ for the surface roughness. Besides, several models and simulations^{11,16,17} assuming restrictive lateral relaxation or lateral relaxation without interlayer diffusion of adatoms also predict the $\beta \approx 0.50$. The observed β_S insinuates that many diffusion processes for the relaxation of the adatoms can be hardly activated at 140 K. It is noteworthy that such a large $\beta \approx 0.50$ has also been observed during homoepitaxial growth of Ag on Ag(111) below 300 K due to the restricted interlayer diffusion¹⁸.

Due to the restricted relaxation of the Fe adatoms at 140 K, the Fe film is expected to contain non-negligible amount of vacancies in it. The formation of vacancies or voids in the growing film has been reported in the metal homoepitaxy at low temperature^{19,20,21,22}. Then, the roughening of the interface may be ascribed to those vacancies and their island formation. The difference between the mobility of the adatom and that of the vacancy seems to be the origin of the different roughening kinetics observed at the surface and the interface.

We examine the thermal stability of the Fe film in the ambient temperature that is usually requested for the device application. After depositing the Fe film of 23 Å at 140 K, the sample is annealed up to 300 K, and then its structure is investigated by XRR. In Fig. 3(a), the overall intensity of the XRR is enhanced by the annealing, and the modulation of the intensity with respect to q_z improves compared with that for the as-grown sample at 140 K, *e.g.* that for 19 Å film in Fig. 1, indicating that the roughness of surface and that of interface are significantly reduced by the smoothing effects at 300 K. Even after two more hours of annealing of the sample, the XRR curve does not show any change (Fig. 3(a)), which should be a sign of the steady state of the system.

In Fig. 3(b), shown is the best-fit XRR curve based on the previously adopted model, the homogeneous single Fe layer on GaAs(100), along with the experimental curve. The theoretical curve does not properly reproduces the experimental one, especially in the high q_z region. Since the interface alloy is expected to form at room temperature, we try to fit the experimental XRR curve, now including the interface alloy inbetween the Fe film and the GaAs substrate. In Fig. 3(b), the best-fit curve from the modified model well reproduces the full experimental data.

The best-fit parameters are as follows; the surface roughness W_S (Vacuum/Fe), an interface roughness $W_{Fe/Interlayer}$ and the other interface roughness $W_{Interlayer/GaAs}$ are 4.58 ± 0.52 Å, 2.89 ± 0.43 Å, and 3.35 ± 0.47 Å, respectively. The interface alloy is 8.64 ± 0.76 Å thick. We assures the reduced roughnesses in comparison with those for the as-deposited Fe films on GaAs(100) at 140 K, *e.g.* that for 19 Å thick film in Fig. 2.

Fig. 3(c) shows the variation of the effective electron density ρ giving the best-fit curve. ρ shows the contribution from the interface alloy of thickness 8.64 ± 0.76 Å between Fe film and GaAs. The mean electron density in this layer is 1.74 ± 0.05 electrons/Å³ that is intermediate between that of Fe (2.14 electrons/Å³) and that of GaAs (1.33 electrons/Å³), reflecting the intermixing of Fe with Ga and/or As.

The limited thickness and the confinement near the interface of the alloy layer should derive from the inefficiency of the bulk diffusion of the Ga and As from the substrate to the overlying film. As a result, the pristine Fe film over this intermixed layer is conserved or kinetically stabilized even at room temperature. In line with the present model, no compound formed by the segregated Ga and As is observed by photoelectron spectroscopy, either¹⁴.

Summary - We investigate the growth of the Fe films on GaAs(100) at 140 K, by UHV *in – situ* x-ray reflectivity. At 140 K, rough Fe film forms on GaAs(100) due to restrictive surface relaxation. The chemical reaction at the interface and surface segregation of As seems virtually suppressed during the growth at 140 K. After warming up the sample to room temperature, intermixed layer of ~ 9 Å forms at the interface, but the system is in a steady state, showing no further development of the interface alloy, keeping the overlying Fe

film in its pristine state.

- ¹ S. A. Wolf, D. D. Awschalom, R. A. Buhrman, J. M. Daughton, S. von Molnár, M. L. Roukes, A. Y. Chtchelkanova, and D. M. Treger, *Science* **294**, 1488 (2001).
- ² J. R. Waldrop and R. W. Grant, *Appl. Phys. Lett.* **34**, 630 (1979).
- ³ M. Zölf, M. Brockmann, M. Köhler, S. Kreuzer, T. Schweinböck, S. Miethaner, F. Bensch, and G. Bayreuther, *J. Mag. Mag. Mat.* **175**, 16 (1997).
- ⁴ H. J. Zhu, M. Ramsteiner, H. Kostial, M. Wassermeier, H.-P. Schönher, and K. H. Ploog, *Phys. Rev. Lett.* **87**, 016601 (2001).
- ⁵ A. Filipe, A. Schuhl, and P. Galtier, *Appl. Phys. Lett.* **70**, 129 (1997).
- ⁶ M. Gester, C. Daboo, R. J. Hickens, S. J. Gray, A. Ercole, and J. A. C. Bland, *J. Appl. Phys.* **80**, 347 (1996).
- ⁷ S. A. Chambers, F. Xu, H. W. Chen, I. M. Vitomirov, S. B. Anderson, and J. H. Weaver, *Phys. Rev. B* **34**, 6605 (1986).
- ⁸ G. W. Anderson, M. C. Hanf, and P. R. Norton, *Phys. Rev. Lett.* **74**, 2764 (1995).
- ⁹ B. D. Schultz, H. H. Farrell, M. M. R. Evans, K. Lüdge, and C. J. Palmstrom, *J. Vac. Sci. Technol. B* **20**, 1600 (2002).
- ¹⁰ Y. Chye, V. Huard, M. E. White, and P. M. Petroff, *Appl. Phys. Lett.* **80**, 449 (2002).
- ¹¹ S. Das Sarma and S. V. Ghaisas, *Phys. Rev. Lett.* **69**, 3762 (1992).
- ¹² L. G. Parratt, *Phys. Rev.* **95**, 359 (1954).
- ¹³ S. K. Sinha, E. B. Sirota, S. Garoff and H. B. Stanley, *Phys. Rev. B* **38**, 2297 (1988).
- ¹⁴ J.-M. Lee, S.-J. Oh, K. J. Kim, S. U. Yang, J. H. Kim, and J.-S. Kim (to be published).
- ¹⁵ A.-L. Barabási and H. E. Stanley, *Fractal Concepts in Surface Growth*, (Cambridge University Press, Cambridge, 1995).
- ¹⁶ Z. Zhang, J. Detch, and H. Metiu, *Phys. Rev. B* **48**, 4972 (1993).
- ¹⁷ S. Das Sarma and P. Tamborenea, *Phys. Rev. Lett.* **66**, 325 (1990).
- ¹⁸ W. C. Elliott, P. E. Miceli, T. Tse, and P. W. Stephens, *Phys. Rev. B* **54**, 17938 (1996).
- ¹⁹ C. E. Botez, W. C. Elliott, P. E. Miceli, and W. Stephens, *Phys. Rev. B* **66**, 075418 (2002).
- ²⁰ C. E. Botez, K. Li, E. D. Lu, W. C. Elliott, P. F. Miceli, E. H. Conrad, and P. W. Stephens, *Appl. Phys. Lett.* **81**, 4718 (2002).

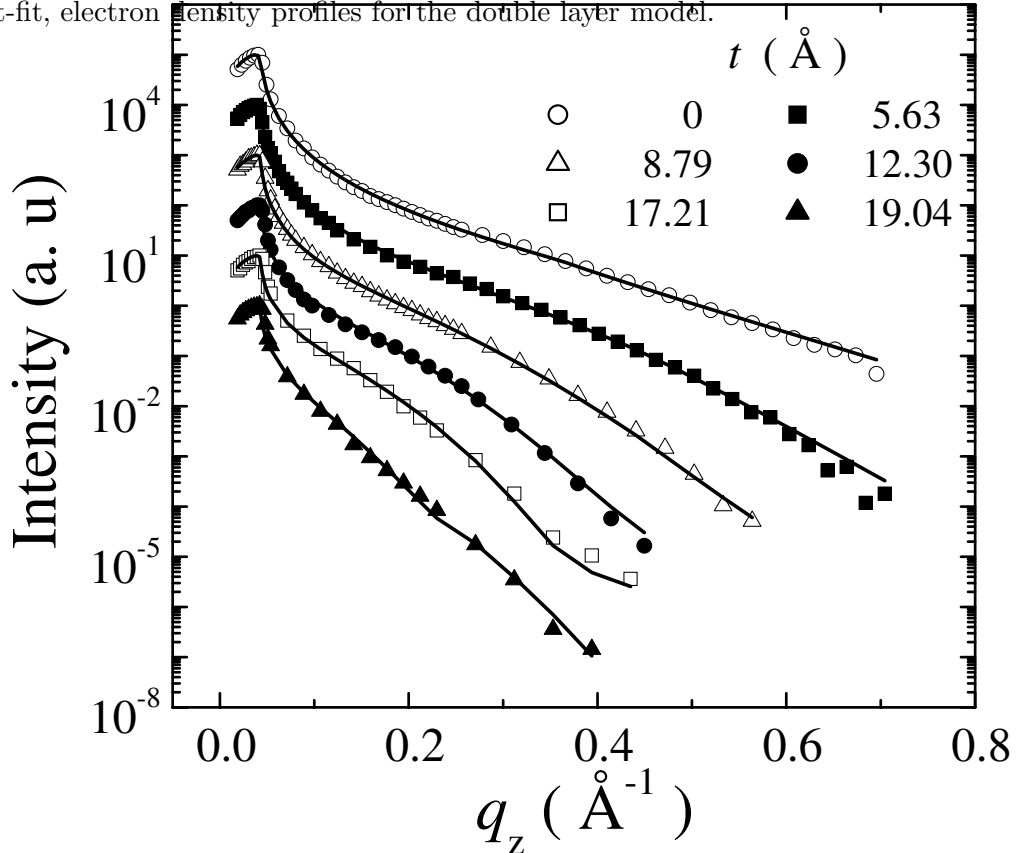
²¹ K. J. Caspersen and J. W. Evans, Phys. Rev. B **64**, 075401 (2001).

²² F. Montalenti and A. F. Voter, Phys. Rev. B **64**, 081401 (2001).

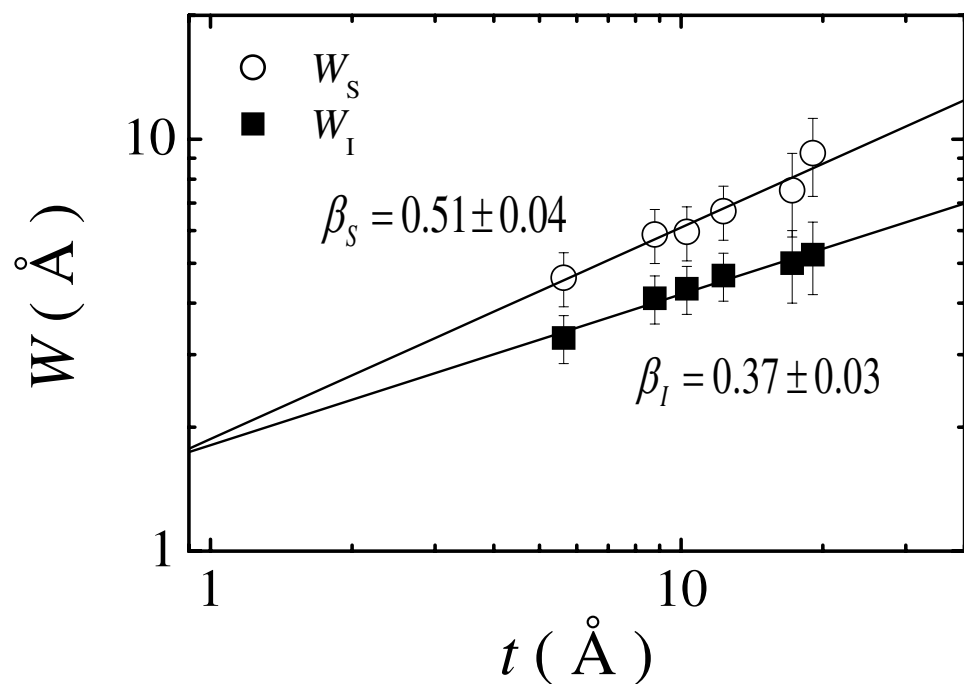
FIG. 1: Specular x-ray reflectivity (symbols) as a function of the out-of-plane momentum transfer, q_z for increasing Fe film thickness, t at 140 K. The solid line is the theoretical prediction by the Parratt's formalism. The curves are vertically shifted with respect to each other for clarity.

FIG. 2: The surface roughness, W_S and interface roughness, W_I as a function of the deposited Fe film thickness, t at 140 K. The solid lines shows the power law fitting results of W_S and W_I with the scaling relation, $W \sim t^\beta$.

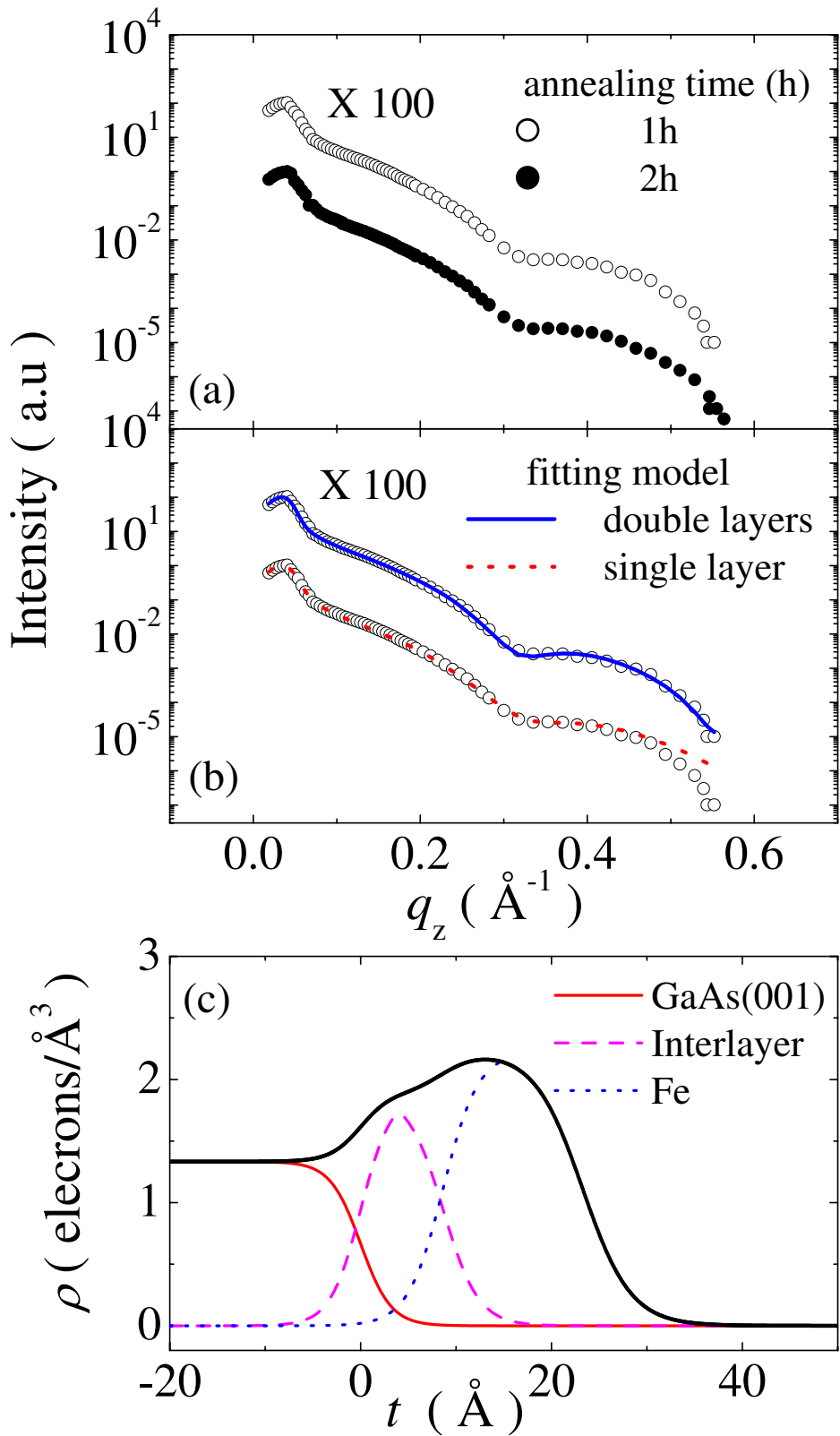
FIG. 3: (a) Specular XRR curves after annealing of 23 Å Fe film at 300 K for 1 (open circle) and 2 hours (solid triangle), respectively. (b) The solid (dashed) line in the upper (lower) graph is the best-fit curve according to the model of homogeneous single Fe layer (an Fe layer and then an alloy layer) on GaAs(100). The two graphs are vertically shifted for the clear presentation. (c) the best-fit, electron density profiles for the double layer model.



Kim *et al.* Fig. 1



Kim *et al.* Fig. 2



Kim *et al.* Fig. 3
10